Electrical Power and Energy Systems 155 (2024) 109540

Contents lists available at ScienceDirect

International Journal of Electrical Power and Energy Systems

journal homepage: www.elsevier.com/locate/ijepes

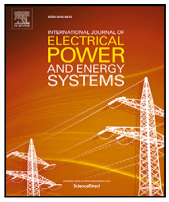

Analysis of the simultaneity factor of fast-charging sites using Monte-Carlo simulation

Finn Silber [a], Stefan Scheubner [b], Alexandra Märtz [a,*]

[a] Karlsruhe Institute of Technology, Institute for Industrial Production, Chair of Energy Economics, Hertzstraße 16, Karlsruhe, 76187, Baden-Württemberg, Germany
[b] EnBW AG, E-Mobility Division, Durlacher Allee 93, Karlsruhe, 76131, Baden-Württemberg, Germany

ARTICLE INFO

Keywords:
Electric mobility
Charging infrastructure
Monte–Carlo simulation
Simultaneity factor

ABSTRACT

Given the increasing number of battery electric vehicles, the availability of suitable fast-charging infrastructure is crucial. However, designing such sites requires enough capacity in the electric power grid. A major influencing factor on the effect of fast-charging sites on the power grid is the simultaneity factor, i.e. the share of installed power related to the theoretical maximum power. The aim of this work is to investigate optimal simultaneity factors for fast-charging sites depending on various influencing factors. Real-world charging data from the biggest German operator is used in a stochastic approach via Monte-Carlo Simulation. It was found that in most cases, fast-charging sites can be designed with a simultaneity factor of 0.5 to satisfy demand. Applying this would reduce the effect on the power grid as well as reduce costs and time to build charging infrastructure. In consequence, the demand of the rising electric vehicle number can be met more efficiently.

1. Introduction

The share of electric vehicles (EVs) worldwide rises constantly in recent years. This trend is strongly driven by policy makers in their efforts to reduce greenhouse gas emissions and is therefore likely to continue. With increasing EV sales, the public charging networks must expand as well. Thereby, high-power charging and thus a short charging duration is crucial for the acceptance of electric mobility [1].

However, the additional power demand causes stress on the local power distribution grid. The ability of the grid to include the capacity for EV charging is a widespread concern in the general public [2–4]. In consequence, high grid-upgrade costs are projected by recent studies [5,6].

When evaluating the additional stress on the power grid exerted by fast-charging sites, the so-called simultaneity factor is of great importance: the relation between the actual available power at the site and the theoretical maximum [7]. Preparing the grid for the theoretical maximum and reserving the capacity all time is a great task and official government programs are based on that requirement, e.g. in Germany [8]. However, in reality charge point operators (CPOs) design their charging sites with lower simultaneity factors creating lower stress on the grid.

Aforementioned studies [5,6] use certain assumptions about the simultaneity factor to calculate the effect of electric vehicle (EV) charging on the grid. However, the simultaneity factor depends on various complex influence factors and not many publicly accessible charging data sets exist for evaluation. On the other hand, its influence can be drastic: if charge point operators (CPOs) would design their sites with a simultaneity factor of 0.5, the strain on the electric grid is only half of the theoretical maximum.

This work aims to perform an analysis on the magnitude of the simultaneity factor based on real-world data from a German CPO. The goal is to identify appropriate simultaneity factors based on charging demand for different scenarios. Thereby, several influencing factors are investigated and their effect on the simultaneity factor is assessed using a Monte-Carlo approach. To this purpose, the following research questions are explored in this paper:

- **RQ1:** How do the influence factors geographic location, number of arriving EVs, number of charging points and type of charging station influence the performance of a charging site and the optimal simultaneity factor ψ_{opt}?
- **RQ2:** Can energy storage systems increase the performance of a charging site and help to reduce the simultaneity factor sufficiently to be economical?

The paper is structured as follows. After Section 2 provided a literature review, Section 3 introduces the used methodology before the simulation setup is explained in Section 4. The results of the different scenarios investigated in the Monte-Carlo Simulation (MCS) are presented in Section 5. Lastly, concluding remarks are given in Section 6.

* Corresponding author.
E-mail address: alexandra.maertz@kit.edu (A. Märtz).

https://doi.org/10.1016/j.ijepes.2023.109540
Received 23 March 2023; Received in revised form 16 July 2023; Accepted 27 September 2023
Available online 16 October 2023

2. Related work

The importance of charging infrastructure as a driver for the market ramp-up of EVs and the associated acceptance of EVs has already been frequently investigated in the literature. [9] investigated the background that could lead to a reduction in the acceptance of EVs. The analysis focuses on access to efficient charging. An additional study [10] focuses on the impacts of costs, charging options, and mileage for EVs as well as the customer service quality on the adoption of EVS. [11] examines policy measures to promote the use of EVs and charging behavior in a combined way. In this context, fast charging stations could be identified as crucial to support and enable a high penetration of EVs in the future. This is supported by numerous literature reviews by various authors. [12], who reviewed the existing literature and summarized the findings on the importance of the framework conditions for the need for charging infrastructure. [13] collected and assessed the literature on electric vehicle charging infrastructure. The authors focused on the types of charging infrastructure that exist, the key functions and players in the market, and the future policies needed for a widespread expansion of EVs.

The resulting impact of a high market share of EVs and thus fast-charging infrastructure on the power grid is a known research area. There are even studies on whether EVs and the corresponding charging infrastructure can be used to deliberately attack the power grid [14]. Apart from such extreme situations, the impulsive and stochastic load type induced by EVs can be challenging for the grid. [15] notes that the load characteristics of EV loads can render conventional assessment methods unsuitable. For this reason, the author proposes an algorithm that captures the intertemporal response of the grid assets and enables rapid assessment through an integrated interface. [16] focuses on the spatio-temporal distribution of EV loads, and [17] can also be ranked when assessing the impact of long-range EVs on the overall charging demand, transformer load and voltage quality in a real distribution system. However, detailed and data-based usage profiles of the charging station loads are not included. In addition, when assessing the impact on the grid many studies base their calculations on the installed charging power by CPOs. The fact that lower simultaneity factors are used in practice is often disregarded and in other cases based on assumptions because not much data is accessible on this.

When public databases are not available, the necessary load profiles are often generated using agent-based models simulating the daily routine of EV drivers, such as in [18]. However, the outcome from such agent-based approaches is strongly influenced by the assumptions of the researchers, e.g. the share of home and public charging [19].

On the other side, researchers address optimal charging site setups from the perspective of a CPO. These setups are usually evaluated in cooperation with peakshaving strategies where renewable energies are used on site. A new probabilistic mixed integer linear programming formulation for determining the optimal capacity and type of renewable generation and energy storage was proposed in [20]. In addition, [21] analyzed the optimal design of an EV fast-charging station taking into account the interplay between renewable energy generation and storage systems. The combined consideration of smart charging strategies for EVs considering several charging options at the charging station can be found in [22]. A component of significant attention is stationary BESSs and especially their economic viability. [23] propose an fast charging system model that considers grid services and battery degradation. The relation of the size of the BESS and the value of the power contracted is evaluated in order to satisfy the needs of EVs and meet the battery state-of-charge limits. In the simulation study of [24], the opportunities to significantly improve the economics of DC-fast charging stations by reducing grid charges were investigated. The analysis results show that demand charges and electricity consumption can be reduced by adding BESS and by using PV. In [25] it is shown, that the application of electrical storage systems (ESS) in fast charging stations can be seen as a way to reduce station operating costs of the station and to reduce the negative impact of the electricity grid. The authors proposed an approach for determining the optimal size of the storage system for a fast charging station. [26] present an approach that uses multi-objective optimization to determine the optimal energy storage capacity for a fast charging station on a trunk road. The results show that their proposed method maintains the voltage drop and maintain the high peak demand with the lowest cost. Hence, [23] and [24] conclude that current battery prices are too high for an economical solution. However, many studies lack large data-sets and mostly focus on the specific component of interest instead of the whole site topology including viable simultaneity factors. Two examples for a studies analyzing the simultaneity factor are [18,19]. Still, it is not evaluated on a charging site level.

In consequence, this paper provides an analysis on the simultaneity factor based on a large charging database. It will be investigated how the charging sites can be right-sized to both meet the demand of EV drivers and minimize the load on the electric power grid.

Nomenclature

BESS	Battery Energy Storage System
CP	Charge point
CPO	Charge point operator
CS	Charging station
CSD	Charging session database
d	Simulation day
e	Capacity of the BESS
EV	Electric vehicle
k	Number of charging stations
h	Highway site
l	Location type
MCS	Monte-Carlo Simulation
n	Number of EVs arriving at a CP per day
p	Maximum power of the charging stations in the MCS
$P_{\mathrm{c,max}}$	Maximum charging power of an EV
P_{CS_i}	Maximum power of charging station i
P_d	Power demand at the charging site
P_{lb}	Lower bound of the generated charging curve
P_T	Maximum power of the transformer
q_{BESS}	SOC of the BESS
q_{end}	SOC at the end of the charging process
q_{start}	SOC at the beginning of the charging process
RCD	Real charging data
RQ	Research question
S	Simulation scenario
SOC	State of charge
t_a	Arrival time of an EV
u	Urban site
VRD	Vehicle registration database
α	Acceptable power reduction
Δ_ω	Performance difference between scenarios
Θ_{EV}	Charging curve of an EV
ψ	Simultaneity factor
ψ_{opt}	Optimal simultaneity factor
ω	Share of power reduction at the site
ω_d	Share of power reduction for a day
ω_t	Share of power reduction for a minute
ω_S	Share of power reduction for a scenario

3. Methodology

3.1. Overview

The main components of a fast-charging site are the transformer with the connection to the power grid and the charging stations (CSs), as illustrated in Fig. 1.

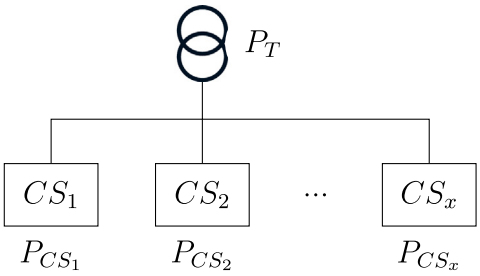

Fig. 1. Illustration of the charging site setup.

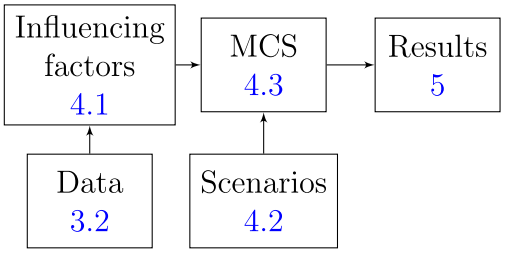

Fig. 2. Block diagram providing the section overview.

Each individual CS_i offers electric power of P_{CS_i}. The power P_T to operate the entire charging site then comes from the transformer. The relation between transformer power and accumulated power of all charging stations x is given by the simultaneity factor ψ:

$$\psi = \frac{P_T}{\sum_{i=1}^{x} P_{CS_i}} \tag{1}$$

A simultaneity factor of 1 means all chargers are being operated at maximum power P_{CS_i} and thus the transformer capacity is used 100%. The determination of the simultaneity factor ψ has far-reaching impacts, especially for the CPO as well as for the sustainable integration of EVs in general. Setting ψ too high leads to unnecessary costs for the CPO with regard to the grid connection and to the hardware. In this case, the consequence would be an over-dimensioning of the charging-site and at the same time, an over-calculated capacity in the grid and is thus associated with limitations in the charging infrastructure expansion. On the other hand, too low values for ψ mean that the charging site is under-dimensioned. Hence, the entire demand of EVs at the site cannot be met which means a restriction of the customers' charging behavior and, in turn, a potential decrease in user acceptance.

In this work, optimal values for the simultaneity factor ψ_{opt} shall be identified using real charging data and a MCS. The approach is illustrated in Fig. 2 and consists of several steps.

At first, real charging data is required for this analysis. These data are presented in the following Section 4.1. Subsequently, the actual analysis can be executed starting with the identification of influencing factors on charging behavior. These are presented in Section 4.1 and include for example the number of EVs arriving each day or the maximum available power per charging point.

To answer the research questions introduced before, several scenarios are defined in Section 4.2. With those scenarios and the influencing factors, a stochastic simulation approach via MCS is executed, shown in Section 4.3. Finally, the results with regard to site performance are presented in Section 5.

3.2. Data and hardware

In this work, real charging data (RCD) is used for the simulation to ensure realistic charging scenarios. The data was from the charging network of EnBW in Germany and is presented in Table 1. Charging sites clustered as *highway* are located in areas within five minutes of a highway. Other charging sites are mainly positioned on urban parking lots of retail partners such as supermarkets. The charging data consists of information shared between the individual charging stations and the CPO backend via the Open Charge Point Protocol (OCPP). It comprises operating parameters, customer information and measurement values such as current charging power.

Table 1
Data from a fast-charging network.

	Count
Total chargers	922
Total charge points	1,437
Highway chargers	303
Highway charge points	446
Total charging sessions	~500,000

Table 2
Assumed costs for components and grid connection.

Position	Value	Unit
Power station	100	[€ kW^{-1}]
Annual grid fee	18	[€ $(kWa)^{-1}$]
Grid connection	100	[€ kW^{-1}]
BESS ≤ 100 kWh	1,000	[€ kWh^{-1}]
BESS > 100 kWh	500	[€ kWh^{-1}]

EnBW mostly uses charging station hardware by the manufacturer Alpitronic, called Hypercharger [27]. It is available in two versions with a maximum power of 150 or 300 kW and has two charge-points each. In the case of two parallel charging sessions at a singular charging station, the maximum available power is split between the two EVs. Since the RCD mostly originates from Hyperchargers, this hardware is also used in the simulation presented in Section 4.

For a CPO, an important motivation to lower ψ is the cost reduction of the charging site. In order to also include the costs in the analyses, the costs for the components presented in Table 2 are assumed. The grid connection prices are taken from a German grid operator [28]. The lifetime for the transformer and BESS is estimated to be 20 and 10 years, respectively. An inflation of 1.5% was defined for the calculation.

4. Simulation setup

4.1. Influencing factors

To choose ψ_{opt} for a fast-charging site, the demand at the charging stations must first be assessed. Overall, the demand is defined by arriving EVs that need to be charged. Thereby, the distribution of their arrival times t_a decides how many parallel charging sessions take place simultaneously. The distribution of arrival times for the simulation runs can be extracted from RCD presented in Section 3.2.

The actual amount of power required by a single EV at a given time depends on the EV model specific charging curve Θ_{EV}. The curve in turn depends on the state of charge (SOC) values q_{start} at the beginning and q_{end} at the end of the charging process, each can be taken from the RCD. The distribution of EV models is publicly accessible from the official vehicle registration database (VRD) in Germany [29]. For the sake of simplicity, it is often assumed for analyses that charging takes place with a constant charging power over the entire charging duration. However, the charging curve in reality is not constant but depends on various parameters such as battery age, SOC or battery temperature. To account for such effects, in this work a measure of uncertainty is introduced to the charging curves. Thus, they are sampled from a predefined probability function following the approach in [1]. The theoretical charging curve is taken from the EV model specification under the assumption that the maximum charging power $P_{\text{c,max}}$ is

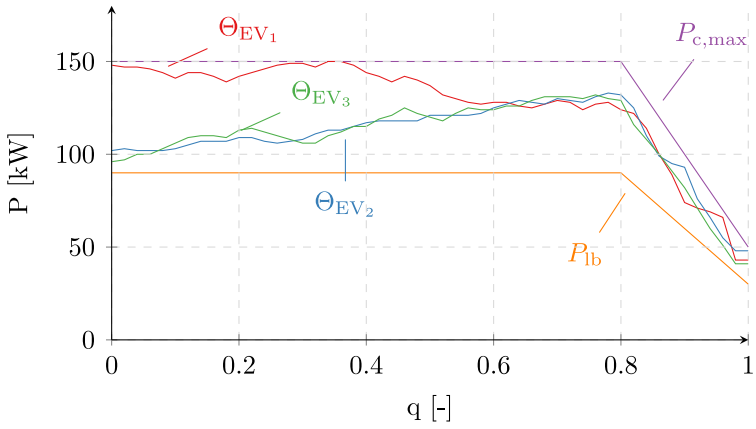

Fig. 3. Three exemplary charging curves of the *Audi S E-tron Quattro* model.

Table 3
Considered influencing factors for the power demand of a fast-charging site.

Influencing factor	Variable [unit]	Data origin
Arrival time	t_a [min]	RCD
Starting SOC of EV	q_{start} [%]	RCD
Final SOC of EV	q_{end} [%]	RCD
EV model	EV [–]	VRD
Storage SOC	q_{BESS} [%]	Uniform distribution
Charging curve of EV	Θ_{EV}	Probabilistic model

Table 4
Overview of the scenario variables.

Scenario variable	Symbol [unit]	Values
EVs per CP per day	n [–]	2, 4, 8, 15
Location type	l [–]	highway, urban, all
Number of CS	k [–]	2, 4, 8
Max. power of CS	p [kW]	150, 300, mixed
BESS capacity	e [kWh]	0, 75, 150, 300

available until the SOC of $q = 80\,\%$. An additional lower bound P_{lb} is introduced according to Eq. (2):

$$P_{lb}(q) = 0.6 \cdot P_{c,max}(q) \tag{2}$$

P_{lb} is defined based on several measurements with real test-vehicles where the communicated charging curve of individual vehicles were compared to actual curves in the field. This included both summer and winter times, whereas low charging power could especially be observed in cold environments. The individual charging curves for each arriving EV at the simulated site is sampled from the area between $P_{c,max}$ and P_{lb}, therefore more realistic curves are achieved compared to calculating with the theoretical maximum (see Fig. 3 for an example and [1] for more details).

If the charging site is equipped with a BESS, the related SOC is chosen from a uniform distribution at the beginning of a simulation run. All considered factors are summarized in Table 3.

4.2. Scenarios

To reduce dimensions of the MCS, a set of scenarios S is chosen with predefined variables shown in Table 4. Thereby, the number n of EVs arriving at a charge point (CP) per day can take values between 2 and 15. The extreme scenario of 15 is used to account for days with untypically high demand, such as the start of holidays.

The location-type l of the considered charging site can be either *highway*, *other* types and *all* stations in the data-set. The number of charging stations (CSs) k can range from 2 to 8. Note the fact that each CS is equipped with two charge points (CPs), where the CS types are provided with a maximum power p of either 150 kW or 300 kW. One scenario is simulated with an equal split of both types (*mixed*).

For BESSs, Li-ion batteries are assumed with a C-rate of 1 for charging and discharging. The capacity e is assumed to be between 0 and 300 kWh.

4.3. Monte-Carlo simulation

To analyze the optimal ψ_{opt}, the actual power demand P_d of the customers on a charging site must be evaluated. Depending on the chosen ψ, this power demand can be supplied by the charging site or not. There are multiple factors influencing P_d as shown in 4.1, and some are subjected to uncertainty. Therefore, a MCS is performed to take the stochastic nature of the scenarios into account, e.g. in arrival times of EVs. For general information on MCS, refer to [30].

In general, the simulation calculates the power demand P_d from the n arriving EVs over the course of a day d. Depending on chosen ψ, P_T is determined which is defines whether the demanded power P_d can be met. At the same time, however, it follows that EVs may also be limited in terms of charging power if the charging stations cannot supply the entire demanded power P_d. The share of power reduction ω is calculated as follows:

$$\omega = \frac{P_d - P_T}{P_T}\,. \tag{3}$$

The time-step used in the MCS is one minute, therefore for each minute ω_t can be calculated. The average power reduction on the whole simulated day d is called ω_d and the average on the whole scenario ω_S.

Before the MCS starts, the scenario S must be defined by the variables introduced in Section 4.2. One central factor is the number of arriving EVs n, for which the corresponding arrival times and SOC values must be sampled from the respective distributions. This is called the initialization phase and is explained in Algorithm 1.

Algorithm 1 Initialization of influencing factors in the MCS.

for i in n **do**
  draw EV_i from corresponding VRD
  generate Θ_{EV} from the corresponding model
  draw $t_{a,i}$ from RCD
  draw $q_{start,i}$ from RCD
  draw $q_{end,i}$ from RCD
end for
draw q_{BESS} from uniform distribution

After the initialization process, the input factors are defined and the load curve for the simulation day can be obtained, starting at midnight

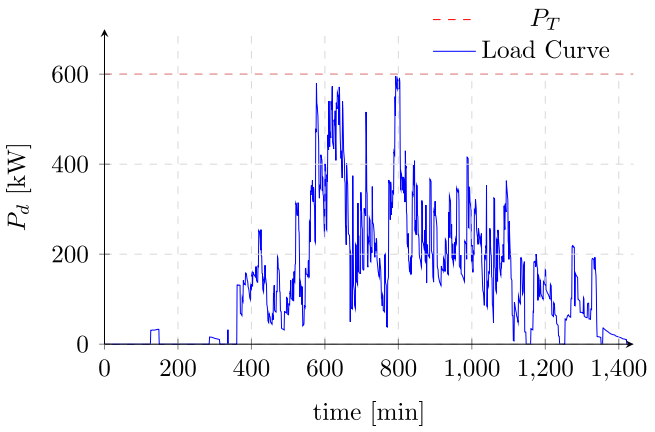

Fig. 4. Exemplary load curve for one day as a result from the MCS with $S(n = 15, l = all, k = 8, p = 150, e = 0)$ and an applied simultaneity factor of $\psi = 0.5$ giving $P_T = 600$ kW.

($t = 0$ min). The simulation first assigns arriving EVs to the respective charging points at the site. If possible, charging points where the EVs can charge with maximum power are selected.

Subsequently, the charging process is simulated for each minute t, i.e. the demand of all EVs shall be met by the CSs. The power split algorithm of the CS on the individual CPs is considered as well, as explained in Section 3.2. If a BESS is installed at the site, power shortage of the site can be mitigated by the battery. Thus, the BESS is used to charge EVs if $P_d > P_T$ and recharges itself in times of $P_d < P_T$. Therefore, q_{BESS} is updated every minute.

Algorithm 2 Load curve calculation.

```
while ω_d not converged do
    for i in d do
        for t ≤ 1440 do
            allocate EVs arriving at t to chargers
            simulate charging process on site
            terminate charging of EVs leaving at t
            update q_BESS
        end for
        calculate ω_{d,i}
    end for
end while
calculate ω_s
```

If vehicles reached their individual q_{end}, they terminate charging and leave the site thus freeing the CP for subsequent arrivals. After reaching midnight again ($t = 1440$ min), the simulation stops and ω_d is obtained.

The whole process is repeated until a convergence of ω_S is reached following standard MCS methodology [30]. In consequence, the conversion criterion determines whether the simulation of an additional day $d + 1$ changes the value of ω_S significantly. Before the conversion criterion is checked, a minimum of $d = 50$ simulations is executed. Then, additional simulations are executed until these additional results change overall ω_S less than 0.0005. ω_S then represents the final result for the defined scenario.

The complete process is illustrated in Algorithm 2. An exemplary illustration of a resulting load curve from the MCS is shown in Fig. 4. It shows the total power demand of all vehicles combined P_d on every minute of the simulation day.

5. Results

5.1. Performance measure

For a given scenario S, the simulation is executed for $\psi \in [0.1, 0.2, \ldots, 0.9]$. By defining an acceptable threshold α for ω_S values, a CPO can subsequently obtain the optimal simultaneity factor ψ_{opt} for the respective scenario. An exemplary result can be seen in Fig. 5 where $\alpha = 0.01$ was chosen, which means 1% power reduction is acceptable on average.

ψ_{opt} then represents the intersection between α and S. In this example, apparently setting up a charging site with $\psi_{\text{opt}} = 0.5$ results in enough power supply while at the same time not over-sizing the hardware. In the following of this work, $\alpha = 0.01$ is used as a threshold as well.

5.2. Evaluation of input data

Since the real charging data (RCD) is available with highway labels, one of the first questions is whether the chosen inputs differ between highway and urban sites. For the variables t_a, q_{start} and q_{end} the respective probability density functions can be seen in Fig. 6. Arrival times are distributed very similar in the two site categories as well as starting SOCs. A decreased tendency toward higher q_{end} values in highway sites can be identified.

5.3. Charging site performance

As explained in Section 4, the output of the MCS is the share of power reduction for the different scenarios $\tilde{\omega}_S$, while a scenario S is defined by the variable values from Table 4. By comparing the results to α, the optimal simultaneity factor ψ_{opt} can be identified for each scenario S. For that purpose, a total of 319 352 days in 1944 scenarios were simulated and compared. Because of the high number of results, only the most important ones are presented in the following of this section.

Location-type of the charging site: First, the effects of the geographic location of the charging site on the performance of the charging site and the related optimal simultaneity factor ψ_{opt} are analyzed (RQ1). In Section 4.1, it was shown that the input variables differ only marginally with the major difference being q_{end}. To see whether that has an effect on the result, an exemplary comparison can be seen in Fig. 7. For the selected scenario, the difference between the location types is barely visible.

To investigate whether that holds true for all scenarios, the performance difference

$$\Delta_\omega = |\omega_{S1} - \omega_{S2}| \tag{4}$$

between all results with $S_1(n, l_1 = highway, k, p, e = 0)$ and $S_2(n, l_2 = rest, k, p, e = 0)$ was calculated. The outcome can be seen in Fig. 8. Thus, the influence on the location type on ψ_{opt} of a fast-charging site is insignificant. For this reason, the input data for all locations $l = all$ are used in all further analyses. This led to a larger data base and thus to more robust results.

Number of CSs and EVs: Subsequently, the correlation as well as the effect of the number of charging points per charging station and the number of EVs on the performance of the charging site (RQ1) will be presented. Intuitively, an increasing number of charging stations k leads to a lower ψ_{opt}, while a higher number of arriving EVs n leads to a higher ψ_{opt}. An example $S_{k1}(n = 8, l = all, p = 150, e = 0)$ with varying k is presented in Fig. 9, where the intuition on the dependency of k and ψ_{opt} is confirmed. Highest ψ_{opt} values are obtained with only two charging stations. The typical asymptotic shape of the curves shows by accepting larger values of α, a CPO could reduce ψ_{opt} even further with the risk of more customer annoyance.

A general trend visible can be confirmed for all scenarios $S_{k2}(l = all, p = 150, e = 0)$ by looking at Fig. 10. In addition, the second hypothesis of a correlation between ψ_{opt} and number of EVs n is visible. Notably, only the extreme scenario of $n = 15$ results in $\psi_{\text{opt}} > 0.6$. However, when installing 8 charging stations $\psi_{\text{opt}} = 0.6$ is sufficient again.

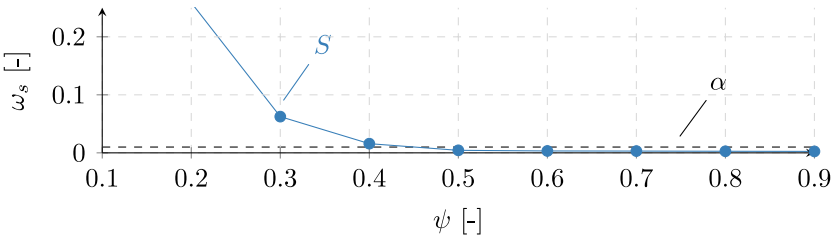

Fig. 5. Exemplary MCS result for a scenario set $S(n = 8, l = highway, k = 4, p = 150, e = 0)$.

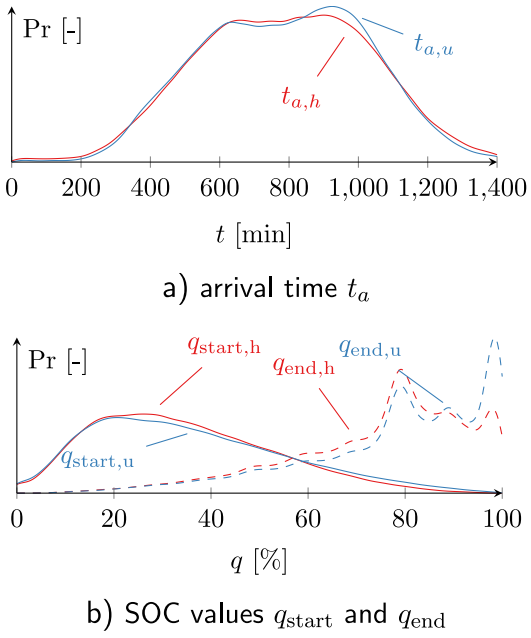

Fig. 6. MCS input variables for highway sites (subscript *h*) and urban sites (subscript *u*) in the RCD.

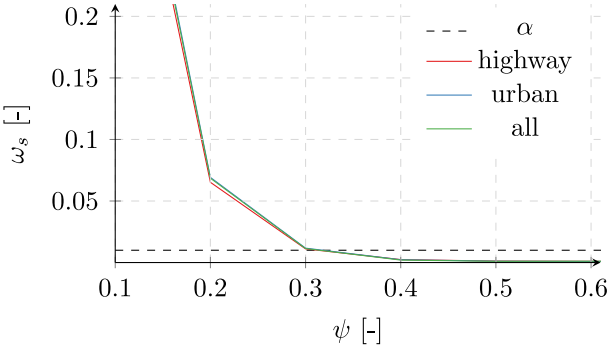

Fig. 7. Performance curves for scenario sets $S_l(n = 4, k = 4, p = 150, e = 0)$ with varying *l*.

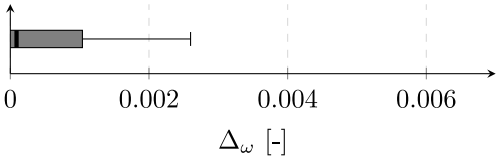

Fig. 8. Boxplot representing the difference in ω_S between scenario sets with $l = highway$ and $l = urban$ for all scenarios with $e = 0$.

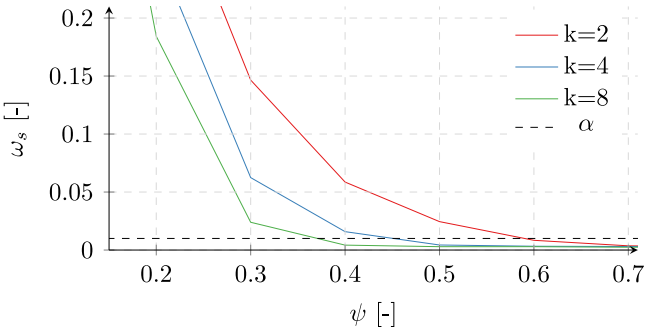

Fig. 9. Performance curves for scenarios $S_{k1}(n = 8, l = all, p = 150, e = 0)$ with varying *k*.

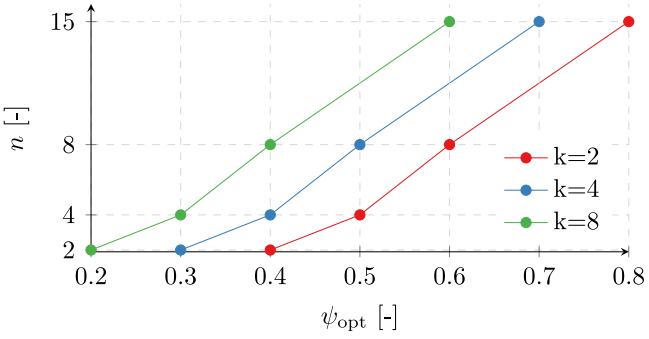

Fig. 10. ψ_{opt} for scenarios $S_{k2}(l = all, p = 150, e = 0)$.

The simultaneity factor of a charging site also has a big impact on the cost calculation. For a charging site with $n = 8$ and $k = 4$, $\psi_{opt} = 0.5$ would be acceptable which means $P_T = 300\,kW$ instead of the full 600 kW in the $\psi = 1$ case. Taking the cost assumptions from Table 2, initial costs can be reduced by 60,000 € for the power station and grid connection with additional savings of 5400 € in annual grid fees. Naturally, such savings grow more important when adding them over several sites within the network of a CPO. From the perspective of a grid operator, the above reduction in P_T means 300 kW less load on the local grid.

Charging station type: In the section above, the relation between ψ_{opt}, *n* and *k* was shown for 150 kW chargers. In the following, the dependence of the performance curve (and thus the simultaneity factor) on the type of charging station is explained. It is likely that increasing maximum power of the hardware leads to decrease in ψ_{opt}. Thereby, also a mix of the charger types is possible, where the considered charging site consists out of $\frac{k}{2}$ 150 kW charging stations and $\frac{k}{2}$ 300 kW charging stations. Since more powerful charging stations are more expensive, it is of interest how much ψ_{opt} can be reduced by using bigger chargers.

Since the application of fewer charging stations *k* represents the scenario with the highest values for ψ_{opt}, $k = 2$ was selected for presentation in Fig. 11. For comparison, the already known results for

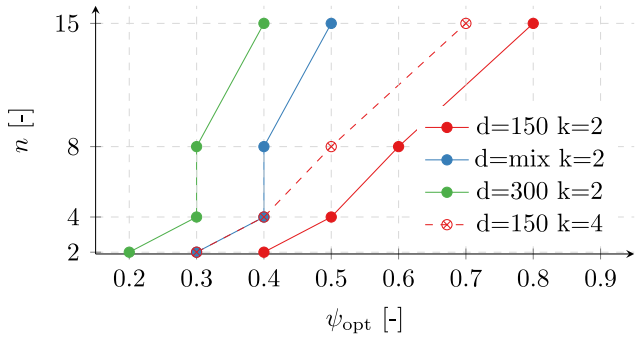

Fig. 11. ψ_{opt} for scenarios $S_p(l = all, k = 2, e = 0)$ with varying p.

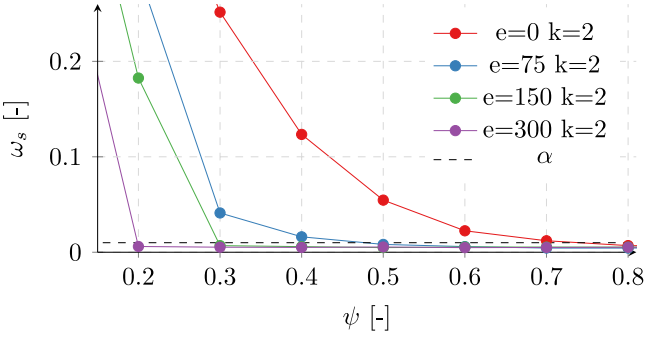

Fig. 12. Performance curves for $S_{e1}(n = 15, l = all, p = 150)$ with varying battery capacity e and number of charging stations k.

$k = 4$ and $d = 150$ kW are shown additionally (Fig. 10). As expected, higher charging power leads to lower ψ_{opt}. In the scenario with $n = 15$, ψ_{opt} can be reduced by 0.3 if one of the chargers offers 300 kW. Note that maximum site power P_T depends on the maximum power of the individual chargers (see Section 3.1).

Battery storage: Here, the effects of BESSs on the charging site performance will be analyzed (RQ2). Installing a BESS at the charging site allows peakshaving and thus the opportunity for reduced ψ_{opt} leading to lower costs for a CPO. Fig. 12 shows an example for scenarios $S_{e1}(n = 15, l = all, p = 150)$ with varying battery capacity e and charging stations k.

As expected, with larger capacity e, the value for ω_S decreases and consequently also ψ_{opt}. Thereby, by comparing the different battery sizes to the $e = 0$ scenario, the peakshaving ability of the batteries compared to a conventional site are visible.

Fig. 13 shows all results for scenarios with $p = 150$ and $l = all$ for the different site sizes. The trend visible in the example above can be confirmed: higher capacity e leads to lower ψ_{opt}. In the $n = 15$ scenario for small sites, installing a large battery reduces ψ_{opt} by 0.6 and even a small battery leads to a reduction of 0.3 (Fig. 13(a)). However, for sites with $k = 8$ chargers, a small battery offers no advantage and the improvement of a large battery is reduced to 0.2 (Fig. 13(b)).

The extra battery on site induces extra costs that need to be compared to the peakshaving opportunity it poses. Table 5 shows the individual business cases for the presented results above using the assumption shown in Table 2. It can be seen that having no battery is usually the cheapest option with one exception ($n = 4, k = 8$ and $e = 75$).

6. Concluding remarks

This work shows how the location-type of a charging site, the number of charging stations, the number of arriving EVs, the type of the charging station and energy storage systems influence the choice of a suitable simultaneity factor. Using a scenario-based Monte-Carlo

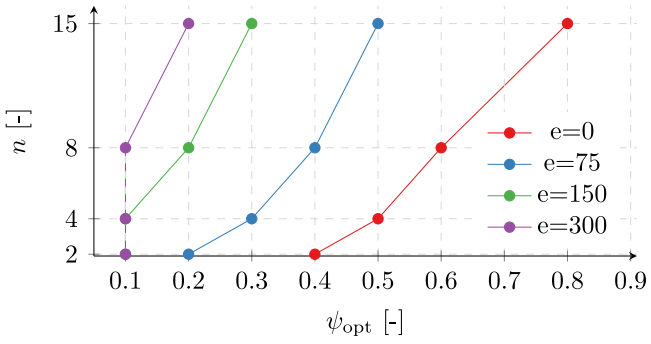

a) ψ_{opt} for scenarios $S_{e2}(l = all, k = 2, p = 150)$.

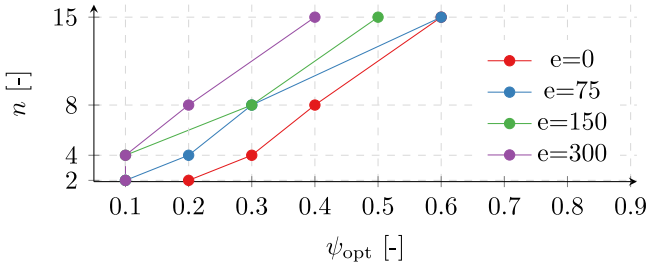

b) ψ_{opt} for scenarios $S_{e3}(l = all, k = 8, p = 150)$.

Fig. 13. ψ_{opt} for BESS scenarios with $d = 150$ and $l = all$.

Table 5
Overview business case for a BESS.

Scenario variables	$e = 0$ [€/a]	$e = 75$ [€/a]	$e = 150$ [€/a]	$e = 300$ [€/a]
n = 2, k = 2, d = 150, l = all	4,500	11,000	9,800	18,500
n = 4, k = 2, d = 150, l = all	5,700	12,100	9,800	18,500
n = 8, k = 2, d = 150, l = all	6,800	13,200	11,000	18,500
n = 15, k = 2, d = 150, l = all	9,100	14,400	12,100	19,700
n = 2, k = 8, d = 150, l = all	9,100	13,300	1,330	22,000
n = 4, k = 8, d = 150, l = all	13,600	17,800	13,300	22,000
n = 8, k = 8, d = 150, l = all	18,100	22,300	22,300	26,500
n = 15, k = 8, d = 150, l = all	27,200	36,000	31,400	35,500

Simulation, performance curves of charging sites with different characteristics were generated. The results are evaluated in the following section.

6.1. Discussion

Based on the results in Section 5, three key findings were identified.

Firstly, the location-type has negligible influence on ψ_{opt}. While the distributions of q_{start} and t_a are much alike between the different location-types, the deviation between the distributions q_{end} for different location-types are not severe enough to have an influence on the performance of a charging site. This was somewhat surprising as a common assumption in the industry is highway sites need more power than urban sites.

Secondly, ψ_{opt} decreases with increasing number of charging stations and ψ_{opt} increases for an increase in arriving EVs. While that was to be expected, the low values for ψ_{opt} in the presented scenarios were surprising. In most cases, a transformer providing only half maximum power of the combined charging stations is enough. That even includes situations with very high demand of 15 arrivals per day per charging point.

Lastly, it was shown that BESS integration leads to reduces simultaneity factors as expected. However, in this work it was economically not feasible. That means potential savings must increase either by

higher prices for power grid connection or lower prices for batteries. Both are expected in the future, i.e. BESS integration might be a good option in the coming years.

6.2. Conclusion and outlook

This work showed the potential for reduced simultaneity factors of fast-charging sites. Adopting it would help in the uptake of electric vehicle charging infrastructure, because on the one hand it means transformers can be smaller and thus power demand of grid operators at the connections points can be lower. This helps energy transmission and does not reserve a maximum amount of power rarely needed which would slow down the build-up of other charging sites.

On the other hand, charge point operators can save resources when designing fast-charging sites and are thus able to build more. This would increase the charging opportunities for drivers and help acceptance of E-Mobility in total.

However, the acceptance threshold α was set to 0.01 which influences the results of ψ_{opt}. In further research, acceptable values for α should be investigated to possibly increase the threshold and further decrease ψ_{opt}. Also, technological advances in charging station design could be integrated as well as improvements in EV charging curves. This would reveal how stable the results of this work prove to be in the face of changing technology. Lastly, the analysis regarding BESS integration can be executed in more detail given the negative results of this publication. Changing C-rates and capacities as well as reducing prices e.g. for second life use can lead to economically feasible solutions.

Declaration of competing interest

The authors declare that they have no known competing financial interests or personal relationships that could have appeared to influence the work reported in this paper.

Data availability

The authors do not have permission to share data.

References

[1] Thorgeirsson AT, Scheubner S, Funfgeld S, Gauterin F. An investigation into key influence factors for the everyday usability of electric vehicles. IEEE Open J Veh Technol 2020;1:348–61. http://dx.doi.org/10.1109/OJVT.2020.3031699.

[2] Englund W. Plug-in cars are the future. The grid isn't ready. 2021, The Washington Post URL https://www.washingtonpost.com/business/2021/10/13/electric-vehicles-grid-upgrade.

[3] Plumer B. Electric cars are coming, and fast. Is the nation's grid up to it?. 2021, The New York Times. URL https://www.nytimes.com/2021/01/29/climate/gm-electric-cars-power-grid.html.

[4] Zhang Y, He J, Ionel DM. Modeling and control of a multiport converter based EV charging station with PV and battery. In: 2019 IEEE transportation electrification conference and expo. IEEE; 2019, p. 1–5. http://dx.doi.org/10.1109/ITEC.2019.8790632.

[5] Hagerty M, Lam L, Sergici S. Electric power sector investments of 75–125 billion dollars needed to support projected 20 million EVs by 2030 according to Brattle Economists. The Brattle Group, Inc.; 2020, https://www.brattle.com/insights-events/publications/electric-power-sector-investments-of-75-125-billion-needed-to-support-projected-20-million-evs-by-2030-according-to-brattle-economists/.

[6] Bermejo C, Geissmann T, Nägele F, Möller T, Winter R. The impact of electromobility on the German electric grid. Mc Kinsey & Company; 2021, URL https://www.mckinsey.com/industries/electric-power-and-natural-gas/our-insights/the-impact-of-electromobility-on-the-german-electric-grid.

[7] Heymann F, Miranda V, Neyestani N, Soares FJ. Mapping the impact of daytime and overnight electric vehicle charging on distribution grids. In: 2017 IEEE vehicle power and propulsion conference. IEEE; 2017.

[8] German Federal Ministry for Digital and Transport. Das deutschlandnetz: Konzept der ausschreibung von 1000 schnellladestandorten auf grundlage des schnellladegesetzes. 2021, URL https://www.bmvi.de/SharedDocs/DE/Anlage/G/deutschlandnetz-konzept-ausschreibung.pdf?_blob=publicationFile.

[9] Engel H, Hensley R, Knupfer S, Sahdev S. Charging ahead: Electric-vehicle infrastructure demand. McKinsey Cent Future Mobil 2018;8.

[10] Sun L, Huang Y, Liu S, Chen Y, Yao L, Kashyap A. A completive survey study on the feasibility and adaptation of EVs in Beijing, China. Appl Energy 2017;187:128–39.

[11] Wolbertus R, Kroesen M, van den Hoed R, Chorus CG. Policy effects on charging behaviour of electric vehicle owners and on purchase intentions of prospective owners: Natural and stated choice experiments. Transp Res D 2018;62:283–97.

[12] Funke SÁ, Sprei F, Gnann T, Plötz P. How much charging infrastructure do electric vehicles need? A review of the evidence and international comparison. Transp Res D 2019;77:224–42.

[13] LaMonaca S, Ryan L. The state of play in electric vehicle charging services–A review of infrastructure provision, players, and policies. Renew Sustain Energy Rev 2022;154:111733.

[14] Sayed M, Atallah R, Assi C, Debbabi M. Electric vehicle attack impact on power grid operation. Int J Electr Power Energy Syst 2022;137.

[15] Mao D, Gao Z, Wang J. An integrated algorithm for evaluating plug-in electric vehicle's impact on the state of power grid assets. Int J Electr Power Energy Syst 2019;105:793–802.

[16] Li M, Lenzen M. How many electric vehicles can the current Australian electricity grid support? Int J Electr Power Energy Syst 2020;117.

[17] Angelim J, Affonso C. Effects of long-range electric vehicles on distribution system using probabilistic analysis. Int J Electr Power Energy Syst 2023;147.

[18] Husarek D, Salapic V, Paulus S, Metzger M, Niessen S. Modeling the impact of electric vehicle charging infrastructure on regional energy systems: Fields of action for an improved e-mobility integration. Energies 2021;14.

[19] Bollerslev J, Andersen PB, Jensen TV, Marinelli M, Thingvad A, Calearo L, et al. Coincidence factors for domestic EV charging from driving and plug-in behavior. IEEE Trans Transp Electr 2021;8(1):808–19.

[20] Moradzadeh M, Abdelaziz MMA. A new MILP formulation for renewables and energy storage integration in fast charging stations. IEEE Trans Transp Electr 2020;6(1):181–98. http://dx.doi.org/10.1109/TTE.2020.2974179.

[21] Domínguez-Navarro JA, Dufo-López R, Yusta-Loyo JM, Artal-Sevil JS, Bernal-Agustín JL. Design of an electric vehicle fast-charging station with integration of renewable energy and storage systems. Int J Electr Power Energy Syst 2019;105:46–58. http://dx.doi.org/10.1016/j.ijepes.2018.08.001.

[22] Moghaddam Z, Ahmad I, Habibi D, Phung QV. Smart charging strategy for electric vehicle charging stations. IEEE Trans Transp Electr 2018;4(1):76–88. http://dx.doi.org/10.1109/TTE.2017.2753403.

[23] Richard L, Petit M. Fast charging station with battery storage system for EV: Optimal integration into the grid. In: IEEE power and energy society general meeting. 2018.

[24] Yang L, Ribberink H. Investigation of the potential to improve DC fast charging station economics by integrating photovoltaic power generation and or local battery energy storage system. Energy 2019;167.

[25] Negarestani S, Fotuhi-Firuzabad M, Rastegar M, Rajabi-Ghahnavieh A. Optimal sizing of storage system in a fast charging station for plug-in hybrid electric vehicles. IEEE Trans Transp Electr 2016;2(4):443–53.

[26] Boonseng T, Sangswang A, Naetiladdanon S. Optimal design of battery-supported fast-charging systems on Australian highways. In: 2022 IEEE transportation electrification conference & expo. IEEE; 2022, p. 935–40.

[27] Alpitronic. Hypercharger by Alpitronic. Alpitronic GmbH; 2022, URL https://www.hypercharger.it/.

[28] GmbH NB. Veröffentlichungen Netzentgelte. 2021, URL https://www.netze-bw.de/unternehmen/veroeffentlichungen#1-1-2.

[29] Federal Motor Transport Authority of Germany (KBA). Statistics on vehicles registered in the central vehicle register on a key date. 2021, URL https://www.kba.de/DE/Statistik/Fahrzeuge/Bestand/ListeHerstellerTypSchluesselnummern/typschluesselnummern_node.html.

[30] Thomopoulos NT. Essentials of Monte Carlo simulation. New York, USA: Springer; 2013, http://dx.doi.org/10.1007/978-1-4614-6022-0.